Electronic Supplementary Material (ESI) for Journal of Materials Chemistry A.

Supporting information

Thermoplastic multiple-functional polysiloxane-based materials from broad gradient-transition multiphase separation

Jianfeng Fan[1], Jiarong Huang[1], Mengwen Yan[1], Zhou Gong[1], Liming Cao[1*], Yukun Chen[1*]

1. Lab of Advanced Elastomer, South China University of Technology, 381 Wushan Road, Tianhe District, Guangzhou 510640, China

*Corresponding Author: Yukun Chen, Email: cyk@scut.edu.cn,
Liming Cao, Email: caoliming324@163.com.

SI.1. Supplementary Figures

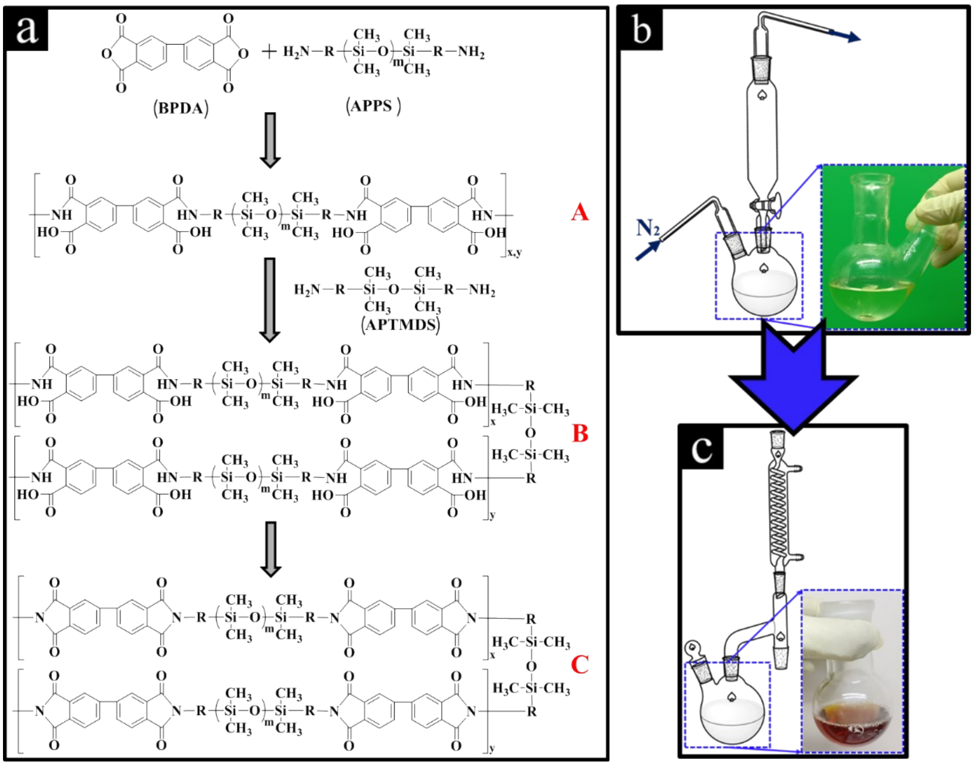

Fig. S1. Schematic route to synthesize PISi copolymers (a), schematic illustration of a reaction device used in the polycondensation reaction (b) and the imidization process (c).

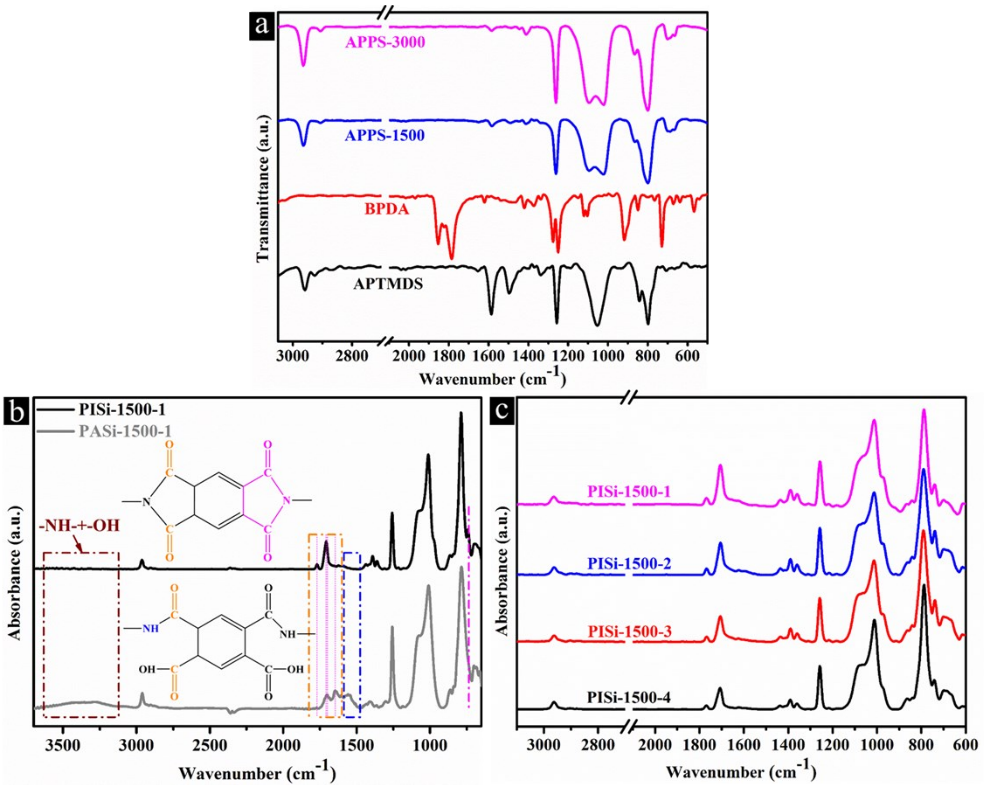

Fig. S2. FT-IR spectra of starting materials (a), the imidization of PASi-1500-1 transformed into PISi-1500-1 (b), and the resulting polymers of PISi-1500 (c).

The FT-IR spectra of APPS exhibit characteristic absorption peaks at about 1095 cm^{-1} (asym Si-O-Si stretching), 1026 cm^{-1} (sym Si-O-Si stretching) and 800 cm-1 (Si-C stretching), as shown in Fig. S2a. The detection of these absorption bands in the resulting poly(imide siloxane) polymers is indicative of the presence of polysiloxane segments (Fig. S2b and 2c).

The imidization reaction was monitored by FT-IR. As shown in Fig. S2b, no residual resonance in the absorption bands at about 1540 and 3278 cm^{-1} was observed, indicating the absence of amide NH. Meanwhile, two new peaks at about 1380 cm^{-1} and 725 cm^{-1} assigning to the vibrations of cyclic imides appeared in the FT-IR spectra after the reaction. Besides, the imidization reaction also can be confirmed by the disappearance of these absorption peaks at 1716 cm^{-1} (C=O of acid group stretching) and 1656 cm^{-1} (C=O of amide group stretching), and the appearance of the absorption bands at about 1773 cm^{-1} (asym C=O of imide group stretching), 1725 cm^{-1} (sym C=O of imide group stretching), respectively. [1-3]

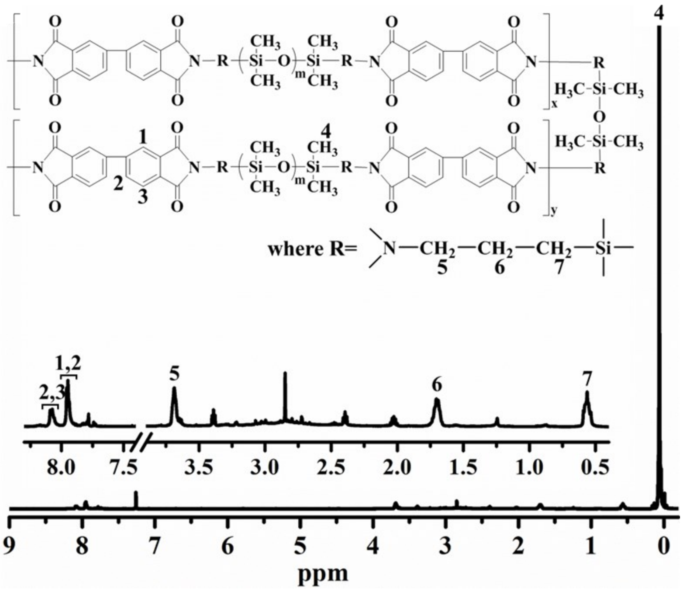

Fig. S3. ^{1}H NMR characterization of PISi-1500-4.

^{1}H NMR characterization of PISi-1500-4 is shown in Fig. S3 [4]. As for PISi, the peaks at 7.96~7.98, 8.03~8.11 and 8.19 ppm are ascribed to the aromatic protons (H1, H2 and H3), respectively; also the peaks at 0~0.08, 0.08~0.14, 0.53~0.57, 3.66~3.69 ppm are detected, representing the protons in methyl group (H4) and methylidyne group (H7, H6, H5), respectively, demonstrating that poly(imide siloxane) polymers have been successfully synthesized. Meanwhile, no residual resonance in the region 9~11 ppm of amide NH protons is observed, which further demonstrates the imidization.

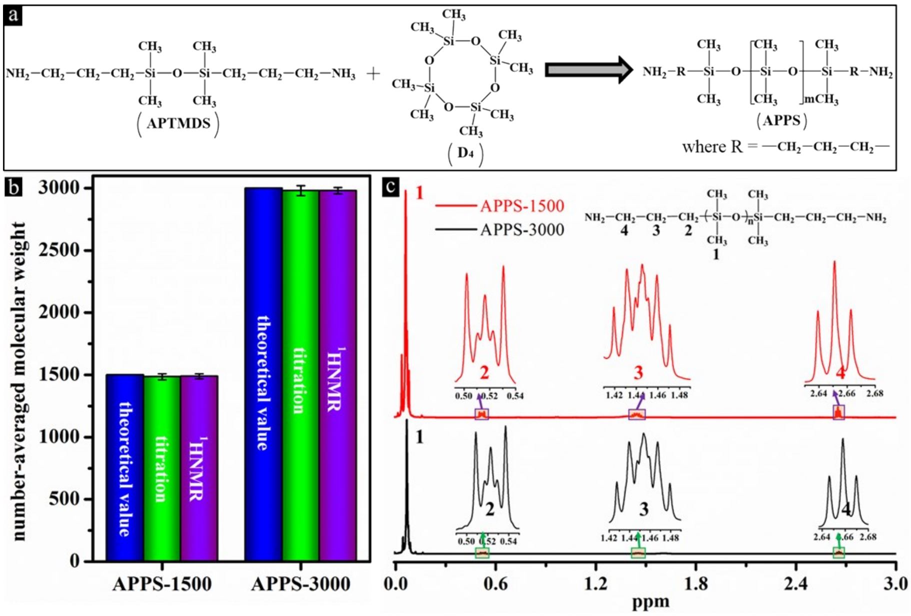

Fig. S4. Schematic route to synthesize APPS (a), and their corresponding number-average molecular weights determined by theoretical calculation, ^{1}H-NMR spectrum and titration of amine-end groups (b), ^{1}H NMR spectra of the NH_2-terminated APPS (c).

By adjusting a different stoichiometric imbalance of D_4 and APTMDS, APPSs with various *n* were obtained, and their corresponding *n* were determined by ^{1}H-NMR spectrum and titration of amine-end groups. The result are shown in Fig. S4b.

^{1}H NMR were used to investigate the structure of APPS-1500 and APPS-3000, as shown in Fig. S4a. ^{1}H NMR of APPS ($CDCl_3$, ppm): 0.04-0.07 ($=Si\text{-}(C\underline{H}_3)_2$), 0.49-0.54 ($=Si\text{-}C\underline{H}_2\text{-}CH_2\text{-}CH_2\text{-}NH_2$), 1.41-1.49 ($=Si\text{-}CH_2\text{-}C\underline{H}_2\text{-}CH_2\text{-}NH_2$), 2.63-2.67 ($=Si\text{-}CH_2\text{-}CH_2\text{-}C\underline{H}_2\text{-}NH_2$).

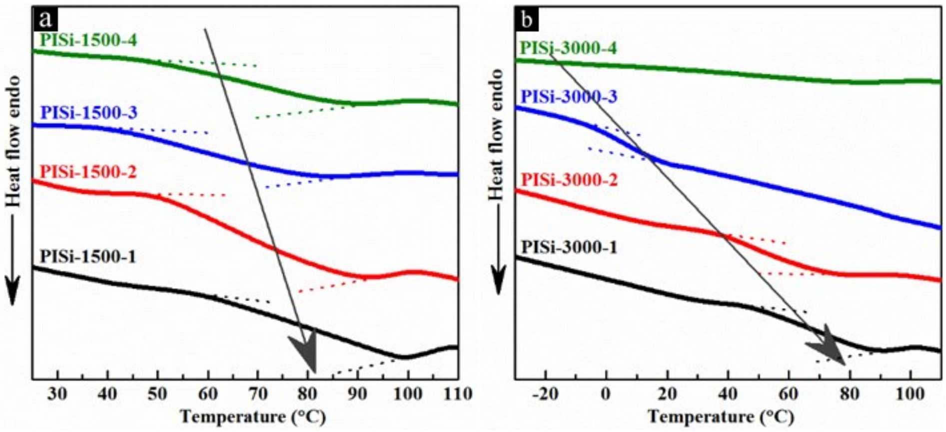

Fig. S5. To corroborate the appropriate phase separation of PISi copolymer, DSC thermal graphs of PISi-1500 (a), PISi-3000 (b) were conducted: the second-heating curves of PISi copolymers with a heating rate of 20 ºC/min.

It is generally believed that multi-glass transition temperatures is a direct evidence of phase separation. As confirmed by others, T_g of the polysiloxane soft block is at about ~-123 ºC [5,6], and as such, the higher T_g in Fig. S5 is ascribed to the hard polyimide segments. For comparison, PISi-3000-4 has no T_g transition in the testing-temperature range and may be regarded as homogeneous phase, which may be due to the sufficient driving force only when the hard segment content reaches to a sufficient level [7].

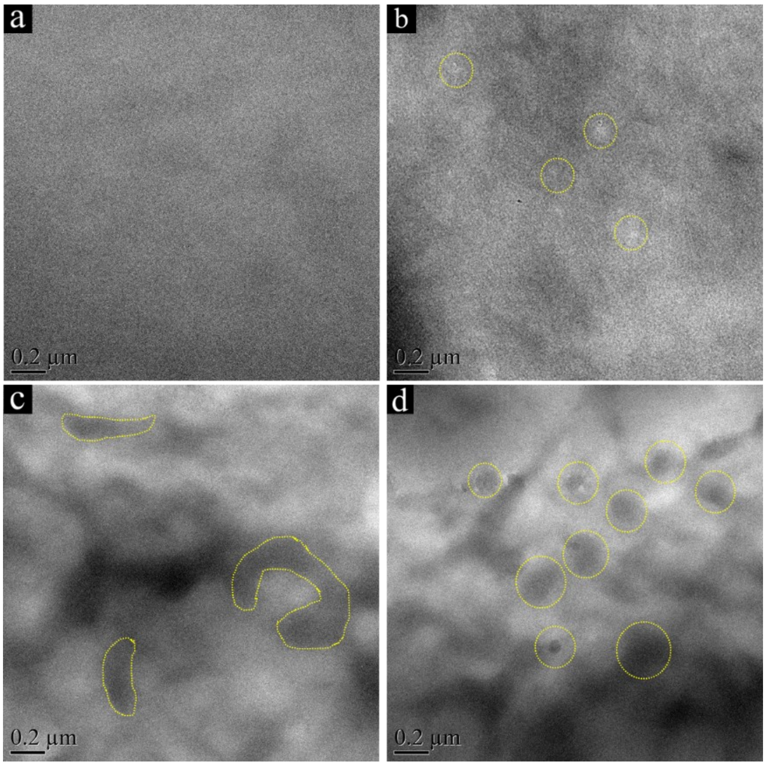

Fig. S6. TEM images of PISi-3000-4 (a), PISi-3000-3 (b), PISi-3000-2 (c) and PISi-3000-1 (d), highlighting the morphology transformation from homogeneous structure to micro-phase separation (scale bar: 200 nm).

It ought to be accentuated that the hard segments containing the strong intermolecular interactions (dipole-dipole interaction and π-π stacking) have a tendency to self-assemble. The TEM phase images of PISi-3000-4 in Fig. S6a do not show clear micro-phase separated morphology. PISi-3000-3 forms many bright spots, like the twinkling stars blossoming in the blackness, demonstrating the hard aggregates. With the hard block content increases, these hard aggregates are sufficiently linked to form long strips due to the shortened distance, suggesting a co-continuous-like structure in Fig. S6c. Finally, more polysiloxane segments are excluded from the polyimide phase due to the stronger intermolecular interactions, resulting in the targeted phase separation (Fig. S6d), in which flexible nonpolar polysiloxane segments curl up and are uniformly distributed in the hard polyimide matrix.

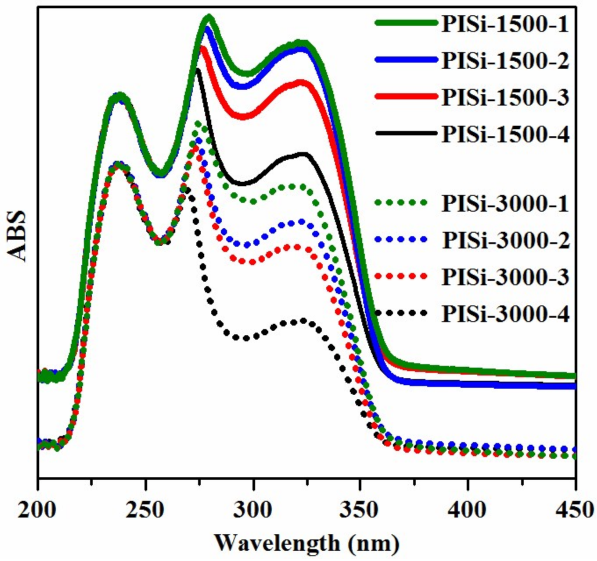

Fig. S7. UV-vis spectra of PISi-1500 and PISi-3000.

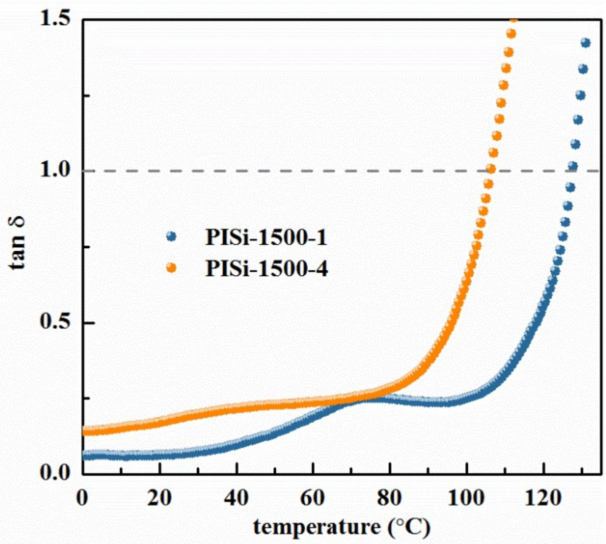

Fig. S8. The loss tangent versus temperature curves determined by DMA under the shear model.

As discussed in other documents [8-11], tan $\delta > 1$ is an indicator for the melt processability of the block copolymers, and its corresponding temperature is defined as the flow temperature (T_{flow}). Therefore, the as-prepared PISi copolymers can be prepared into specimens by hot-pressing (melt processability) at their appropriate temperature, as shown in Fig. S9a.

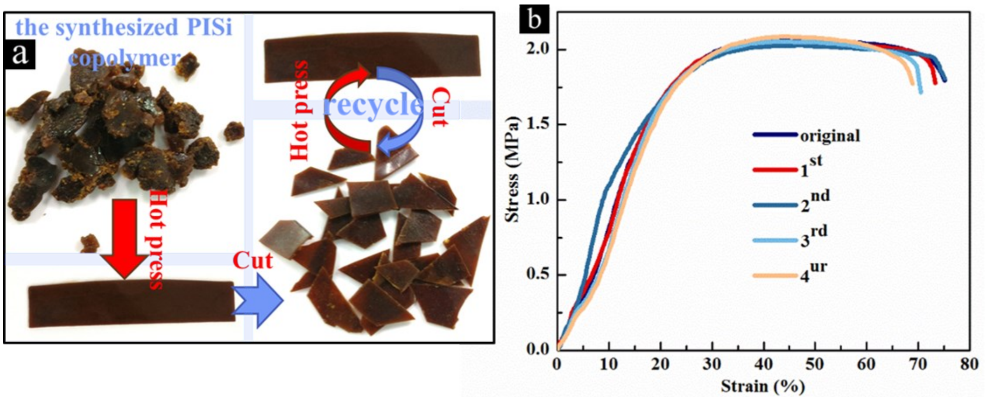

Fig. S9. Image presentation for the reprocessing of PISi-1500-4 copolymer by hot pressing (a), representative stress-strain curves of original and recycled PISi-1500-4 (b).

The PISi-1500-4 specimens were cut into small pieces and then hot-pressed again (Fig. 9a), and tensile tests were employed to evaluate its recycling ability (Fig. 9b).

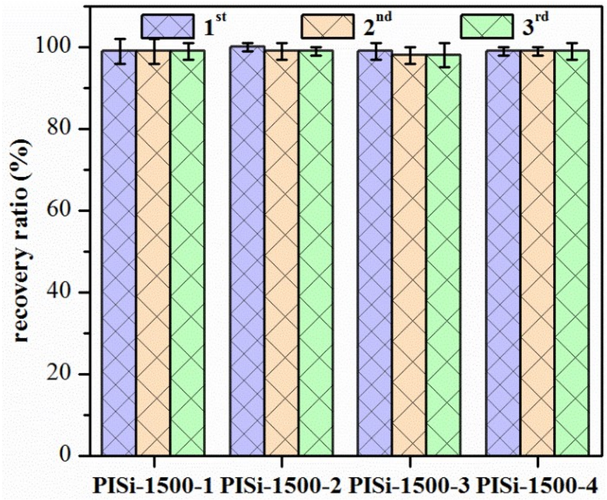

Fig. S10. Recovery ratio of tensile strength for the three times recycling.

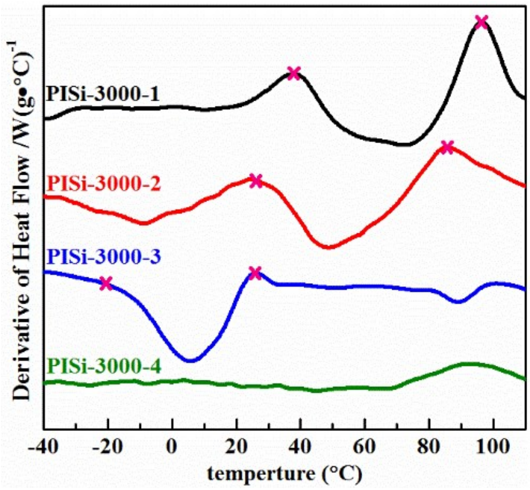

Fig. S11. The derivative of heat flow-temperature curves of the various PISi-3000 copolymers.

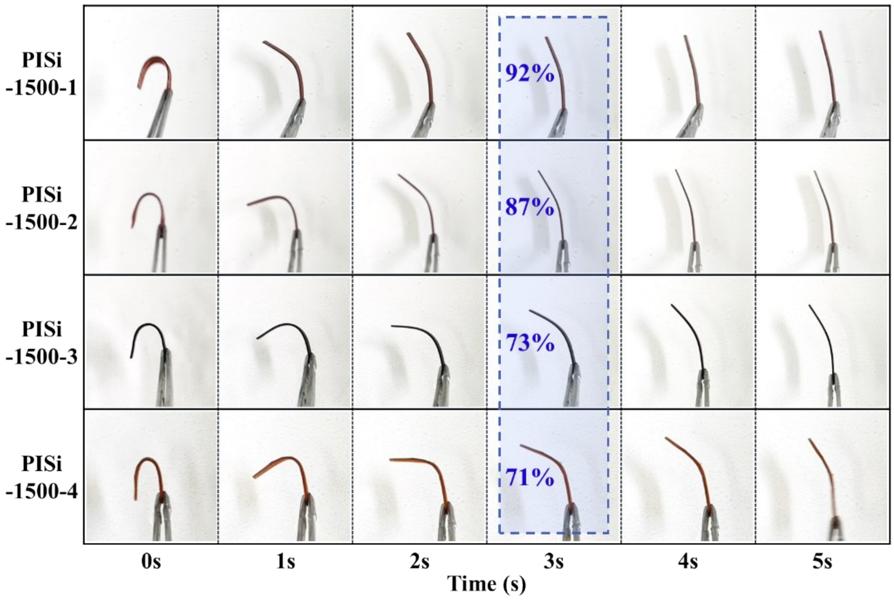

Fig. S12. Frame-by-frame analysis of the shape recovery at T_g+5 ºC.

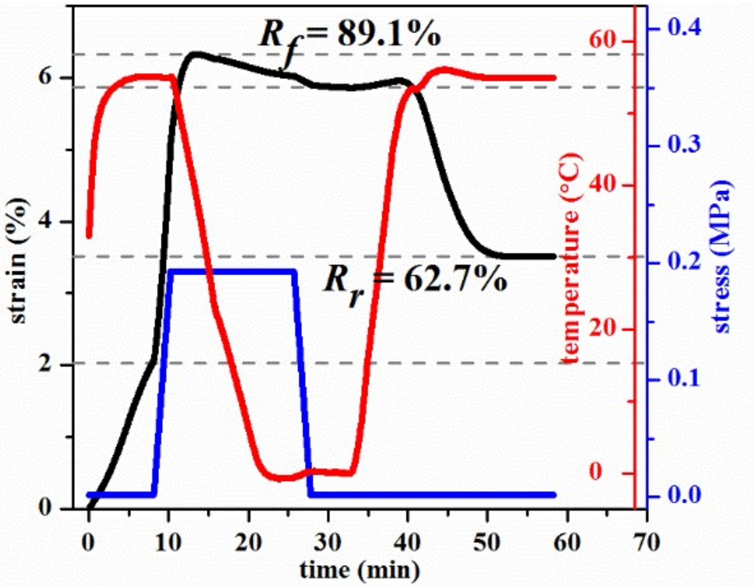

Fig. S13. Thermomechanical analysis of the shape-memory properties of PISi-3000-1.

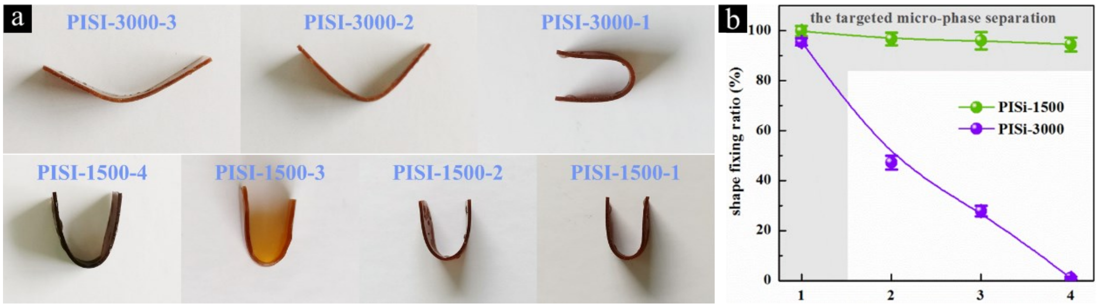

Fig. S14. Shape fixation at room temperature for 24 h after samples fixed in a 20 ºC bath (a), shape fixity ratios at room temperature upon fixation for 24 h (b).

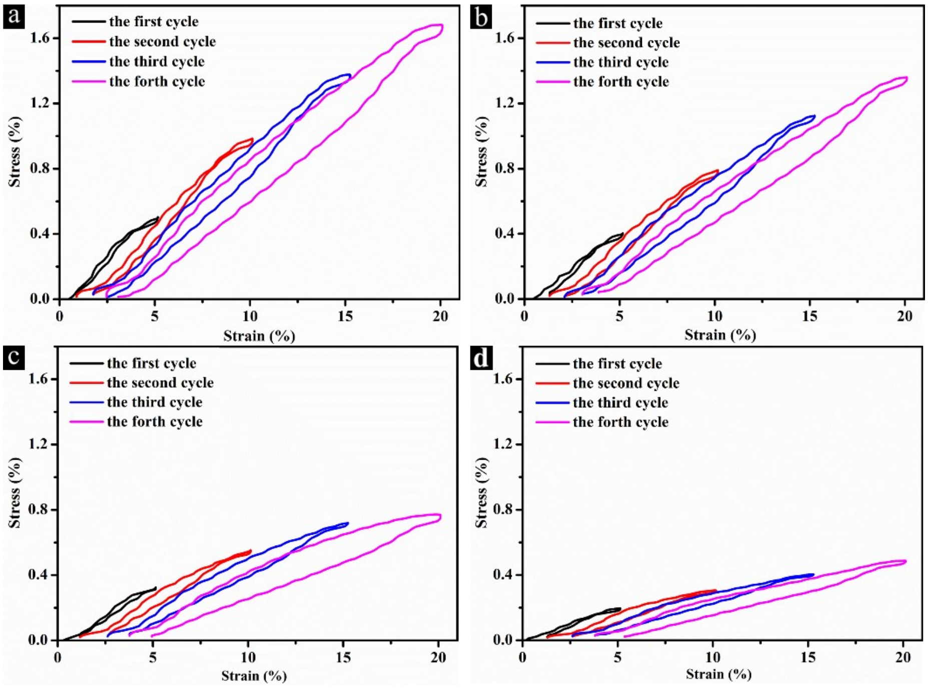

Fig. S15. The high-temperature cyclic tensile curve of and PISi-1500-1 (a), PISi-1500-2 (b), PISi-1500-3 (c) and PISi-1500-4 (d).

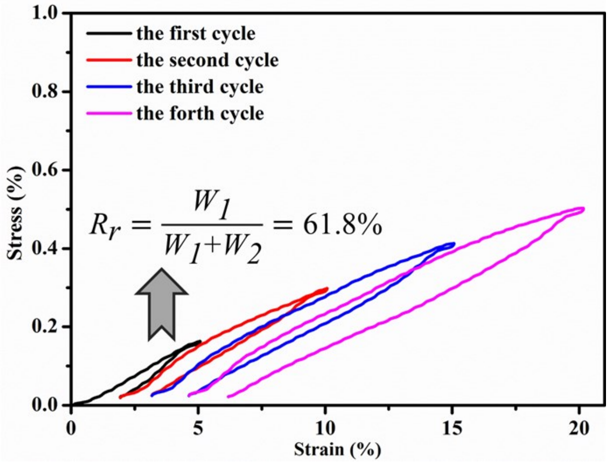

Fig. S16. The high-temperature cyclic tensile curve of and PISi-3000-1.

SI.2. Supplementary Tables

Table S1. Feed ratios, the hard-segment content of PISi.

Sample code	BPDA [mol]	APTMDS [mol]	APPS [mol]	Hard-segment content [wt%]
PISi-1500-1	2.7	1.7	1	29.24%
PISi-1500-2	2.2	1.2	1	26.47%
PISi-1500-3	1.7	0.7	1	23.01%
PISi-1500-4	1.2	0.2	1	18.56%

PISi-3000-1	2.7	1.7	1	18.85%
PISi-3000-2	2.2	1.2	1	16.40%
PISi-3000-3	1.7	0.7	1	13.62%
PISi-3000-4	1.2	0.2	1	10.38%

Reference

1 L. Leimhofer, B. Baumgartner, M. Puchberger, T. Prochaska, T. Konegger, and M. M. Unterlass, *J. Mater. Chem. A*, **2017**, 5, 16326.

2 M. Yoonessi, Y. Shi, D. A. Scheiman, M. Lebron-Colon, D. M. Tigelaar, R. A. Weiss, and M. A. Meador, *ACS nano*, **2012**, 6, 7644.

3 X. L. Xiao, D. Y. Kong, X. Y. Qiu, W. B. Zhang, F. H. Zhang, L. W. Liu, Y. J. Liu, S. Zhang, Y. Hu, and J. S. Leng, *Macromolecules*, **2015**, 48, 3582.

4 X. L. Pei, G. F. Chen, J. T. Liu, and X. Z. Fang, *Polymer*, **2015**, 56, 229.

5 C. H. Li, C. Wang, C. Keplinger, J. L. Zuo, L. Jin, Y. Sun, P. Zheng, Y. Cao, F. Lissel, C. Linder, X. Z. You, and Z. Bao, *Nat. Chem.*, **2016**, 8, 618.

6 P. F. Cao, B. Li, T. Hong, J. Townsend, Z. Qiang, K. Xing, K. D. Vogiatzis, Y. Wang, J. W. Mays, A. P. Sokolov, and T. Saito, *Adv. Funct. Mater.*, 2018, **28**, 1800741.

7 J. Xu, V. Mittal, and F. S. Bates, *Macromolecules*, 2016, **49**, 6497.

8 Y. Meng, W. J. Xu, M. R. Newman, D. S. W. Benoit, and M. Anthamatten, *Adv. Funct. Mater.*, 2019, **29**, 1903721.

9 H. Zhang, Y. Z. Wu, J. X. Yang, D. Wang, P. Y. Yu, C. T. Lai, A. C. Shi, J. P. Wang, S. X. Cui, J. F. Xiang, N. Zhao, and J. Xu, *Adv. Mater.*, 2019, **31**, 1904029.

10 C. S. Boland, U. Khan, G. Ryan, S. Barwich, R. Charifou, A. Harvey, C. Backes, Z. Li, M. S. Ferreira, M. E. Möbius, R. J. Young, and J. N. Coleman, *Science*, 2016, **354**, 1257.

11 T. Wang, Y. Zhang, Q. C. Liu, W. Cheng, X. R. Wang, L. J. Pan, B. X. Xu, and H. X. Xu, *Adv. Funct. Mater.*, 2018, **28**, 1705551.